The implementation of the Klemp–Durran–Bougeault radiative upper boundary condition in the LM with consistent time-split numerical scheme

Almut Gassmann
Hans-Joachim Herzog

Meteorological Institute, University of Bonn, Germany
German Weather Service, Potsdam, Germany

LM User Seminar 2006, Langen

Outline

Motivation – Upper Boundary Condition

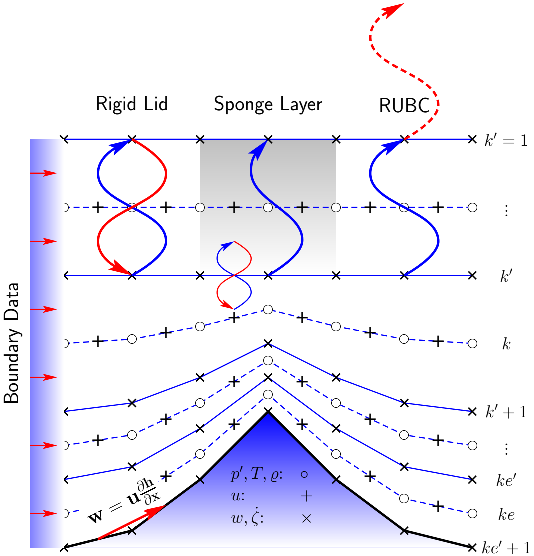

- Rigid lid ($w = 0$) with a sponge layer
- Spurious reflections
- "Useless" grid points
- Upper boundary values sometimes inaccessible

Alternative
↓
RUBC

Physical constraint at the upper boundary

Waves propagating upwards may be approximated as hydrostatic gravity waves with $\omega = \pm \frac{Nk}{m}$ which gives us

$$\hat{w} = \frac{k}{N\varrho} \hat{p}'$$

in Fourier–space at the upper boundary for outward radiating energy (group velocity $\frac{\partial \omega}{\partial m} > 0$).

This condition is local in time and global in horizontal space.

But our model is:

nonhydrostatic	$\omega = \pm \frac{Nk}{\sqrt{k^2+m^2+\frac{1}{4H^2}}}$
compressible	sound waves ?
nonlinear, inhomogeneous	wave solutions ?
limited area	periodicity ?
rotating sphere	Coriolis effects ?

Historical Development

- Klemp and Durran (1983)
  - Application to a (non)hydrostatic (non)linear shallow(deep) atmosphere model without(with) Coriolis effects
  - Not suitable for Rossby waves
  - Implementation in an explicit numerical scheme
- Bougeault (1983)
  - Boussinesq hydrostatic model
  - Implementation in an implicit numerical scheme
  - Accounting for nonperiodicity by adding buffer zones
- Herzog and Binder (1995)
  - Implementation into the EM/DM/SM
  - Filtering of high frequent noise
  - Detrending of FFT-input fields
  - Operational use at SMA (Switzerland), and in versions of Hirlam and Eta models

Historical development for the LM

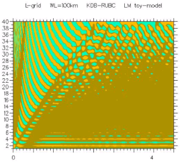

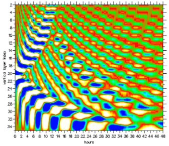

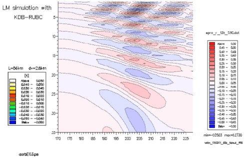

Toy model (isothermal fast-waves model) studies successful with 2 methods:

1. Incorporation of the RUBC into the vertical implicit solver of the fast–waves system (internal method).
2. A direct method independent of a given time scheme (external method).

LM studies only partly successful with method (2).

Reasons for failure in the LM ... and resort

1. The internal method (1) failed due to incomplete gravity wave representation in the fast-modes system. Fast-waves subsystem solved for quasi–base-state ($p_0, T = const$) conditions.
   $\rightarrow$ ALM fast-waves equations solve for the current slow background state
2. The external method (2) relies on a back-lagging crudely interpolated pressure field which is not consistent with the implicit solution method.
   $\rightarrow$ Prefer method (1)
3. The usually applied upper layers are too thick for resolving wave structures. Waves were reflected before reaching the top.
   $\rightarrow$ Redefine layer geometry

Method (1) for the ALM

ALM vs. LM: fast waves | slow modes

$$\frac{\partial p'}{\partial t} - w\frac{1}{\sqrt{G}}\frac{\partial p_0 + p'}{\partial \zeta} + \frac{c_{pd}}{c_{vd}} pD = -\vec{v}_h \cdot \nabla_h p' + Q_p$$

$$\frac{\partial T'}{\partial t} - w\frac{1}{\sqrt{G}}\frac{\partial T}{\partial \zeta} + \frac{1}{c_{vd}}\frac{p}{\varrho} D = -\vec{v}_h \cdot \nabla_h T + Q_T$$

3-diagonal matrix equation:

$$B_2 w_2^{\nu+1} + C_2 w_3^{\nu+1} = D_2 + \mu p'^{\nu+1}_{k'=2}$$

$$A_{k'} w_{k'-1}^{\nu+1} + B_{k'} w_{k'}^{\nu+1} + C_{k'} w_{k'+1}^{\nu+1} = D_{k'} \quad k' \in [3, ke'-1]$$

$$A_{ke'} w_{ke'-1}^{\nu+1} + B_{ke'} w_{ke'}^{\nu+1} = D_{ke'} - C_{ke'} w_{ke'+1}^{\nu+1}$$

Grid staggering:

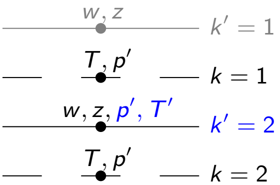

Method (1) for the ALM continued

Gaussian elimination algorithm gives

$$w_2 = F_2 + G_2 {p'}_{k'=2}$$

This is unfortunately nonlinear! Linearize G_2 and apply Fourier-transform and RUBC:

$$\hat{w}_2 = \hat{F}_2 + \bar{G}_2 \hat{p'}_2 = \hat{F}_2 + \bar{G}_2 \frac{\overline{N\varrho_2}}{K} \hat{w}_2, \quad K = \sqrt{k^2 + l^2}$$

At this point we get

$$\hat{w}_2 = \frac{K \hat{F}_2}{K - \overline{N\varrho_2}\bar{G}_2}$$

Back in grid point space that is the appropriate boundary condition for w.

Fourier or Cosine transform?

Problem for real data: no periodicity, low frequency variablility

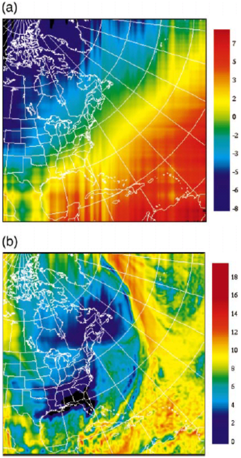

Fig. 3. (a) Trend component that is removed from the humidity field (Fig. 1) to get the (b) detrended field used as input for the detrending-DFT method. The line pattern is not generated by a printing problem but by the detrending itself.

Denis et al., 2002, MWR 130, 1812-1829

FFT on de-trended fields ⟵ ⟶

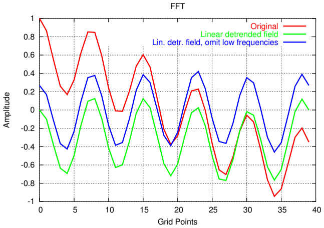

Discrete Cosine Transform, DCT ⟶

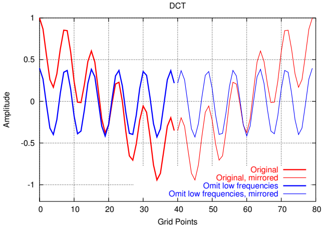

Filtering

To avoid nonlinear instabilities, a filter is applied to the vertical velocity field and the temperature field.
Filter function in Fourier space:

$$\frac{1}{1 + 0.1\tan(\frac{K\Delta x}{2})}$$

w(m/s), incr=0.03m/s

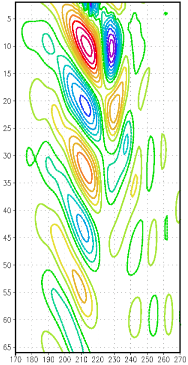

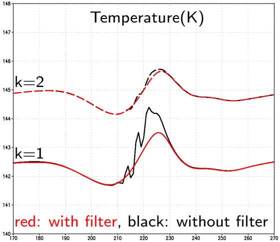

$\Delta x = 500m$, $\Delta z = 300m$

$\Delta t = 8s$, $hstop = 5h$

w(m/s), incr=0.03m/s

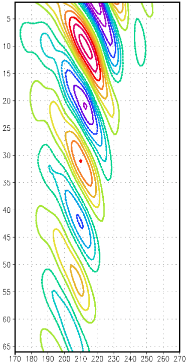

Redefine Layer Geometry

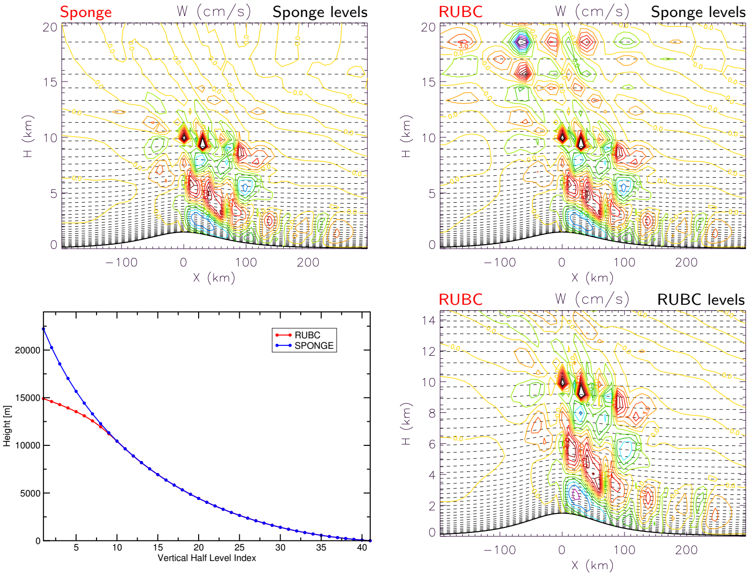

Case study – Initial model adjustment

21 January 2006, 325x325 grid points
Δx=7km, Δt =40s, hstop=24h
Initial data interpolated from GME

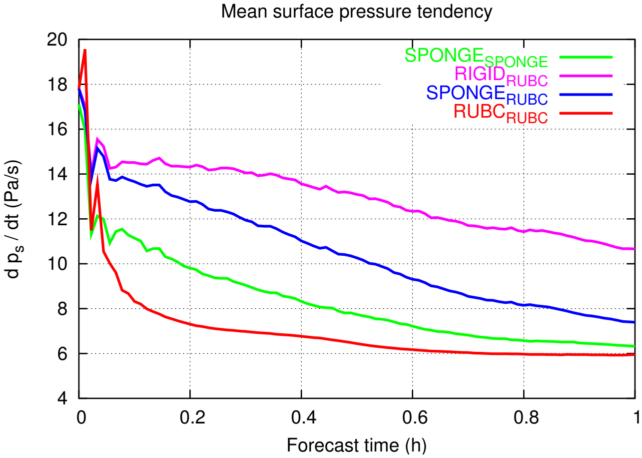

Case study – Surface pressure differences

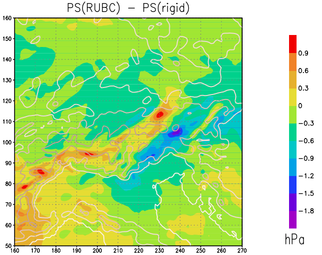

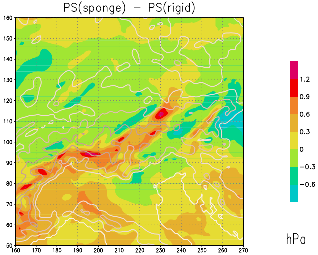

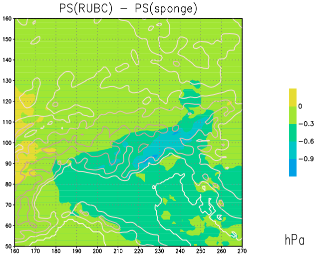

The rigid run uses RUBC levels. No wave pattern is visible in the difference between the RUBC run and the sponge run.

Conclusions

- RUBC successfully implemented!
- Prerequisites:
  - ALM equations
  - Appropriate layer thickness
- Difficulties:
  - Nonlinearity $\longrightarrow$ filtering
  - Nonperiodicity $\longrightarrow$ Discrete Cosine Transform (DCT)
- Real case study is promising!
- To be done: code optimization for DCT